

⁵M. Leventhal and P. E. Havey, Phys. Rev. Lett. **32**, 808 (1974).

⁶C. Fan, M. Garcia-Munoz, and I. Sellin, Phys. Rev. **161**, 6 (1967).

⁷H. W. Kugel, M. Leventhal, and D. E. Murnick, Phys. Rev. A **6**, 1306 (1972).

⁸M. Leventhal, D. E. Murnick, and H. W. Kugel, Phys. Rev. Lett. **28**, 1609 (1972).

⁹F. P. Lawrence, C. Y. Fan, and S. Bashkin, Phys. Rev. Lett. **28**, 1612 (1972).

¹⁰G. W. Erickson, Phys. Rev. Lett. **27**, 780 (1971).

¹¹G. W. F. Drake and R. B. Grimley, Phys. Rev. A **8**, 157 (1973). Equation (9) of this reference is incorrect. It should read

$$\sum_{\theta_2} |Q(\omega_1, \omega_2)|^2 = \frac{1}{4}(|A|^2 + |A'|^2) \sin^2 \theta + \frac{3}{4}|A'|^2 \cos^2 \theta.$$

¹²W. L. Fite, W. E. Kauppila, and W. R. Ott, Phys. Rev. Lett. **20**, 409 (1968); W. R. Ott, W. E. Kauppila, and W. L. Fite, Phys. Rev. A **1**, 1089 (1970).

¹³J. S. Casalese and E. Gerjuoy, Phys. Rev. **180**, 327 (1969).

¹⁴G. W. F. Drake, to be published.

Efficient Positronium Formation by Slow Positrons Incident on Solid Targets*

K. F. Canter, A. P. Mills, Jr., and S. Berko

Department of Physics, Brandeis University, Waltham, Massachusetts 02154

(Received 1 April 1974)

A beam of slow positrons in the few-eV region is directed at bakable solid targets in a vacuum of $(2-4) \times 10^{-8}$ Torr. Measurements of the $2\gamma/3\gamma$ annihilation-yield ratio indicate the conversion of the incident positrons into positronium. The conversion efficiency depends on the target material and incident positron energy, varying from less than 25% at 300 K to 40–85% at 900 K.

In this Letter we report the observation that an external slow-positron (e^+) beam (a few eV) forms positronium (Ps) with high efficiency when colliding with solid targets. The experiment is the first designed explicitly to study the collisions of slow positrons with solid targets, and has been made possible by recent developments in the production of high-flux e^+ beams.¹⁻⁴ The large e^+ -to-Ps conversion efficiency reported here, besides its intrinsic interest, is particularly relevant to the interpretations of recent observations of slow- e^+ emission from metal surfaces,^{4,5} Ps emission from oxide powders,^{6,7} and the intermediate-lifetime component in metal powders.⁸ These phenomena have been observed with fast (≈ 0.5 MeV end-point energy) e^+ that have slowed down internally in the solid, as contrasted to the external-beam technique reported here.

The experimental setup consists of a slow- e^+ beam and a target stage. Slow e^+ are produced in a converter similar to that originally used for e^+ -helium scattering-cross-section measurements.² The converter consists of MgO-coated gold foils, 0.15 mm thick, arranged in a venetian-blind geometry on a 1-cm-diam ring, behind which is placed a ^{58}Co fast- e^+ source. In order to have the target far from the source, the e^+ are magnetically transported through a 1.5-m-long beam tube with a 30° bend in the middle. The tube is baffled internally against fast e^+ and

wound externally with a solenoid; with a field of 75 G, only the slow e^+ are able to reach the target. Approximately one in 3×10^4 of the ^{58}Co e^+ emerge as slow e^+ . The e^+ beam has a measured longitudinal energy distribution of less than 2-eV width, with an intrinsic average energy of 1 to 2 eV with respect to a grounded tungsten grid in front of the converter. The converter can be biased with an accelerating voltage V_A .

Figure 1 shows the details of the target chamber at the end of the beam tube. Pressures at the target range from $(2$ to $4) \times 10^{-8}$ Torr, with a pump-oil-vapor background of less than 10^{-15} Torr. The target cage and target stage can be biased with respect to ground by a voltage V_T . Suitably changing V_A and keeping $V_A - V_T$ fixed, we can keep the incident e^+ energy constant with V_T positive or negative. When tests of target polarity are not being made, the target cage and the grid in front of the cage are removed from the target chamber. Annihilation spectra of the incident e^+ are obtained with a NaI(Tl) detector.

Figure 2 shows the NaI(Tl) pulse-height spectra for 10-eV e^+ incident on a Ti target at 300 and 770 K. The dashed curve labeled "pure 2γ " was obtained by accelerating the e^+ into the Ti target at 300 K with $V_A - V_T = 360$ V. The same spectral shape is obtained by placing a ^{22}Na source surrounded by copper at the location of the target stage. When the Ti target is heated from 300 to

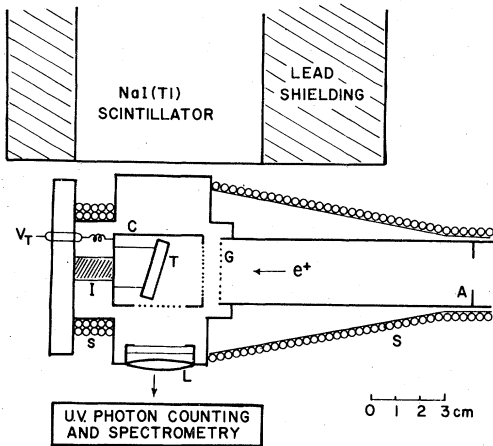


FIG. 1. Target chamber. A, aperture; S, solenoids; G, grounded grid; C, target cage; T, target stage; I, insulator; L, quartz window and lens. C and T are at the same bias V_T . The 3 in. \times 3 in. NaI(Tl) scintillator is coupled to an RCA 8575 photomultiplier. A heater in the target stage allows target specimens to be heated to 900 K.

770 K, a reduction in the 511-keV photopeak accompanied by an increase in the counting rate below 511 keV is observed. We attribute this change to an increase in 3γ annihilation, indicating an increase in freely annihilating Ps formation. At 770 K the photopeak is reduced by 50% compared to the pure- 2γ spectrum, after subtraction of the "beam-off" background. Taking into account the 2γ annihilations from $\frac{1}{4}$ of the Ps formed in the spin-singlet state, and correcting for the probability that two photons from the 3γ annihilations of spin-triplet Ps can enter the scintillator simultaneously and contribute counts under the 511-keV photopeak, the observed 50% photopeak reduction is estimated to correspond to a free Ps formation efficiency ϵ of $(80 \pm 10)\%$. The same analysis yields $\epsilon = (25 \pm 10)\%$ at a 300-K target temperature.

The loss of 2γ annihilations was also measured using two NaI detectors 180° apart. The coincidence rate as a function of target temperature is shown in Fig. 3. Starting with point A (e^+ energy 360 eV, $\epsilon \leq 5\%$) and multiplying the observed fractional loss in coincidences by $\frac{4}{3}$ yields ϵ (23% and 80% for target temperatures of 300 and 750 K, respectively). Estimating the fraction of 3γ annihilations detected in coincidence yields corrected values of ϵ equal to $(25 \pm 5)\%$ and $(85 \pm 5)\%$.

Let us consider the validity of the Ps-formation interpretation of the observed effect of temperature on the single-NaI-detector spectra. The

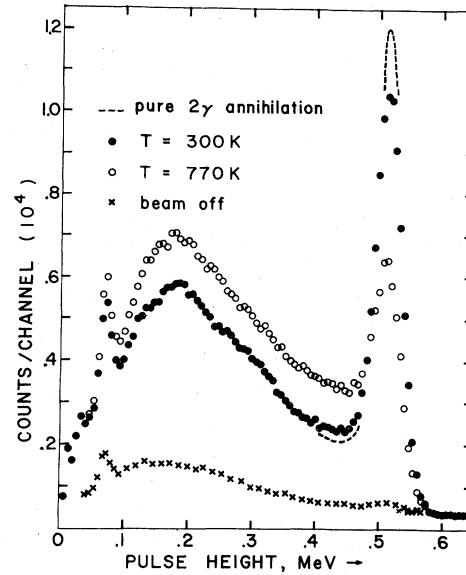


FIG. 2. NaI(Tl) pulse-height spectra of 10-eV e^+ annihilation γ 's from Ti. Run time per spectrum is 80 min, using a 6-mCi ^{56}Co fast- e^+ source. The pure- 2γ spectrum corresponds to no Ps formation.

only other way in which the peak counting rate P at 511 keV might decrease with a simultaneous increase in the valley (between the photopeak and

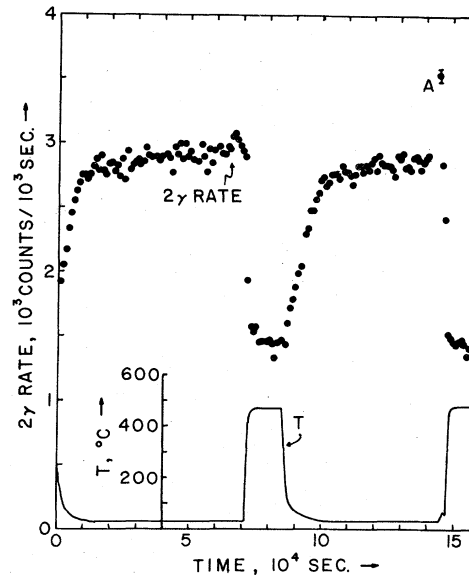


FIG. 3. 2γ -annihilation coincidence rate as a function of target (Ti) temperature for e^+ incident energy of 10 eV. Point A is the coincidence rate for pure 2γ annihilations (no Ps). Note that when the target is cooled, the 2γ rate responds by increasing with a characteristic time of 10^4 sec.

the 340-keV Compton edge) count rate V is for some of the 2γ annihilations to originate from locations out of direct sight of the scintillator, and to undergo Compton scattering into the detector. However, we have found experimentally that the magnetic guiding field constrains the e^+ to annihilate only at the target stage or far back into the beam tube. Further, a pure 2γ source was moved to various positions inside the target chamber in an attempt to simulate a geometry-related reduction in P/V . The largest reduction of P/V achieved was 30%, but at a cost of a 40% reduction in total count rate. In sharp contrast, baking a Ti target, for example, yields a 60% decrease in P/V , accompanied by a 15% increase in total count rate. An increase is to be expected as a result of the higher detection probability for 3γ annihilation.

In lieu of an arrangement of three shielded scintillation detectors (not permitted by the spatial limitations imposed by the pumping system at the target chamber), a second detector with a 2 cm \times 8 cm Pb slit geometry was placed at 90° and 30 cm away from the target. Upon our baking an etched Au target (which shows the same P/V change as does Ti), the coincidence rate between the two counters increased above the 300-K coincidence rate by $0.50 \pm 0.01 \text{ sec}^{-1}$ with a slow- e^+ beam of $6000 e^+ \text{ sec}^{-1}$. This agrees with an estimate of the increase in 3γ annihilations which result in two of the three γ 's being detected, using the values of ϵ given above.

Measurement of the P/V changes with and without the target cage, and a search for 2γ coincidences away from the target, have also been carried out to differentiate between the possibilities of freely annihilating Ps being very weakly bound to the target surface and its actually escaping from the target. Although the results presently indicate that the Ps escapes, the escape velocity cannot be determined until the reflection coefficient of Ps colliding with the interior walls of the target chamber is known. Measurements of the effect of changing the polarity of V_T [while keeping the e^+ incident energy $E_i \approx e(V_A - V_T)$ constant] show that (1) P/V is independent of target polarity, and (2) the fraction of incident e^+ which are reemitted by the target as slow e^+ is less than 10% for $E_i > 10 \text{ eV}$.

The measured values of ϵ (to the nearest 5%) for 10-eV e^+ incident on the targets at 800 K are as follows: Au, etched, 85%; Au, unetched, 60%; Ti, 85%; Cu, oxygen-free high-conductivity, 60%; graphite, pyrolytic single crystal, 70%;

fused quartz (Suprasil), 65%; MgO, single crystal, 75%; Al, 75%; ZnO, powder, 80%; quartz, single crystal, 50%. None of the samples investigated exhibit appreciable changes in ϵ when the target temperature is varied from 750 to 900 K. For all targets at room temperature, ϵ is less than 25% for $E_i > 10 \text{ eV}$. At intermediate temperatures ϵ exhibits a complex dependence on the target's bakeout history. In addition to the thermal effects, ϵ varies with E_i . For example, for Ti at 800 K, ϵ decreases from 85% for $E_i = 10 \text{ eV}$ to 40% for $E_i = 350 \text{ eV}$. At room temperature ϵ decreases from 25% to less than 5% over the same range of E_i . The variation of ϵ with E_i is smaller for Au targets.

We interpret the effect of temperature on the increase in Ps formation to be the result of desorbing the many physisorbed layers of water as well as other possible contaminants typically present on surfaces in nonultrahigh vacuum. However, the baking does not necessarily remove the oxide or activated oxide-hydrocarbon compound layers; thus Ps formation might be due to such nonmetal surface layers, since oxide powders are known to be efficient converters of internally thermalized e^+ into Ps.^{6,7}

A preliminary measurement of ϵ for 10-eV e^+ incident on a special tungsten filament target yields $\epsilon = (80 \pm 5)\%$ at 1800 K. This result perhaps comes closest to indicating Ps formation at a pure metal surface, although at this temperature an oxide layer can still persist on W. Even though Ps formation in bulk metals is forbidden,⁹ formation at metal surfaces might still be possible by virtue of the electron cloud extending beyond the positive-ion background of the metal.¹⁰

To date, slow- e^+ emission has only been observed to be relatively efficient from surfaces having several adsorbed layers of contaminants. Recent measurements show that e^+ emission from metals is reduced significantly upon baking the surfaces at 500 K in a vacuum of 10^{-7} Torr.¹¹ Other experiments show a reduction in the slow- e^+ yield as a function of the length of time that the surfaces have been kept in vacuum.³ Moreover, our results indicate that Ps formation is the dominant low-energy e^+ surface process when most of the adsorbed contaminants are removed by baking. Such effects are consistent with an earlier suggestion that slow- e^+ emission from "metals" at room temperature is a result of dissociated Ps.² However, there may be some fundamental difference in the surface effects between e^+ diffusing to the surface as a result of

thermalization inside the bulk solid and e^+ being introduced externally at low energies. In any case, the interpretation of these effects in terms of pure metal surfaces is premature, and ultra-high-vacuum experiments are needed.

The photon counting system referred to in Fig. 1 is being employed in a search for 2430-Å photons resulting from the Lyman- α transition of the Ps if any is formed in the $n=2$ excited state.¹² If at least 0.1% of the Ps were formed in the $n=2$ state, we would observe a significant signal (95% confidence level) after a 24-h run with our present sensitivity. As of this writing, we have observed no Lyman- α photons for any target material investigated.

The authors wish to acknowledge valuable discussions regarding surface conditions with Dr. E. W. Plummer, University of Pennsylvania, and Dr. J. C. Tracy, General Motors Technical Center.

Note added.—The positronium formation has now also been confirmed by a direct 3γ coincidence measurement. Using an extended target chamber we obtain a triple coincidence rate between three 3×3 -in. NaI(Tl) detectors, 10 cm from a Ti target, of $0.362\pm 0.027\text{ sec}^{-1}$ at 525°C versus $0.064\pm 0.013\text{ sec}^{-1}$ at 30°C with a background rate $\approx 0.017\text{ sec}^{-1}$.

*Work supported by the National Science Foundation and the U. S. Army Research Office, Durham, N. C.

¹P. G. Coleman, T. C. Griffith, and G. R. Heyland, Proc. Roy. Soc., Ser. A **331**, 561 (1973).

²K. F. Canter, P. G. Coleman, T. C. Griffith, and G. R. Heyland, J. Phys. B: Proc. Phys. Soc., London **5**, L167 (1972).

³W. C. Keever, B. Jadaszliwer, and D. A. L. Paul, in *Atomic Physics 3*, edited by S. J. Smith and G. K. Walters (Plenum, New York, 1973), p. 561.

⁴S. Pendyala, P. W. Zitzewitz, J. W. McGowan, and P. H. R. Orth, Phys. Lett. **43A**, 298 (1973).

⁵D. G. Costello, D. E. Groce, D. F. Herring, and J. W. McGowan, Phys. Rev. B **5**, 1433 (1972).

⁶R. Paulin and G. Ambrosino, J. Phys. (Paris) **29**, 263 (1968).

⁷S. M. Curry and A. L. Schwalow, Phys. Lett. **37A**, 5 (1971).

⁸R. Paulin, R. Ripon, and W. Brandt, Phys. Rev. Lett. **31**, 1214 (1973).

⁹H. Kanagawa, Y. H. Ohtsuki, and S. Yanagawa, Phys. Rev. **138**, A1115 (1965), and references therein.

¹⁰N. D. Lang and W. Kohn, Phys. Rev. B **3**, 1215 (1971).

¹¹S. Pendyala, D. M. Bartell, and J. W. McGowan, Bull. Amer. Phys. Soc. **18**, 1505 (1973).

¹²L. W. Fagg, Nucl. Instrum. Methods **85**, 53 (1970), and references therein. Recently two groups [S. L. Varghese, E. S. Ensberg, V. W. Hughes, and I. Lindgren, Bull. Amer. Phys. Soc. **18**, 1503 (1972); S. L. McCall, Bull. Amer. Phys. Soc. **18**, 1512 (1973)] have reported experiments to excite ground-state Ps to the $n=2$ state.

Raman Scattering from Coherent Spin States in n -Type Cds

R. Romestain,* S. Geschwind, and G. E. Devlin
Bell Laboratories, Murray Hill, New Jersey 07974

and

P. A. Wolff†

Department of Physics, Massachusetts Institute of Technology, Cambridge, Massachusetts 02139

(Received 8 May 1974)

When the donor spins in n -CdS are simultaneously irradiated with laser light at frequency ω_L and microwaves at frequency ω_0 near the spin resonance, intense sidebands at $\omega_L \pm \omega_0$ are observed for forward scattering which are more than 3 orders of magnitude greater than those for spontaneous spin-flip Raman scattering. This phenomenon is explained as Raman scattering from coherent states.

We have observed intense sideband radiation at frequencies $\omega_L \pm \omega_0$, when the electron spins in n -CdS are simultaneously irradiated with laser light at frequency ω_L and microwaves at frequency ω_0 , close to the donor-spin resonance frequency. These huge sidebands are observed in the forward direction and are at least 3 orders of

magnitude stronger than those due to spontaneous spin-flip Raman scattering (SFERS). This effect has been seen in crystals ranging in concentration from $(1\text{ to }5)\times 10^{17}$ (excess donors)/cm³. It may be described as coherent SFERS from coherent spin states or, alternatively, as parametric conversion of light via the macroscopic magnetic